Cardiac Beta-Adrenergic Receptor Density Measured In Vivo Using PET, CGP 12177, and a New Graphical Method

Jacques Delforge, André Syrota, Jean-Pierre Lançon, Kénichi Nakajima, Christian Loc'h, Marc Janier, Jean-Marie Vallois, Jérome Cayla, and Christian Crouzel

Service Hospitalier Frédéric Joliot, Commissariat à l'Energie Atomique, Orsay, France; Département d'Anesthésie, Hôpital Bichat, Paris, France; Kanazawa University School of Medicine, Kanazawa, Japan; and INSERM U13, Hôpital Claude Bernard, Paris, France

The in vivo quantification of myocardial beta-adrenergic receptor has been obtained in five closed-chest dogs using positron emission tomography (PET). The ligand was racemic ($\pm$)[^{11}C] CGP 12177, a very potent hydrophilic antagonist of the beta-adrenergic receptor. A kinetic method appeared unsuitable because of the presence of metabolites which made the input function difficult to measure and also inaccurate. Therefore, a graphical method, based on a particular protocol, was proposed. The animals were injected with a trace amount of ($\pm$)[^{11}C]CGP 12177, which was followed 40 min later by a second injection of radioligand with a low-specific activity. An additional injection of an excess of unlabeled CGP 12177 was administered after 90 min and allowed for the estimation of the dissociation rate constant. The main advantage of this graphical approach is that the results are obtained without having to measure the input function and therefore without estimating the metabolites. The average value of B'_{max} was 31 $\pm$ 4 pmole/ml of tissue and the dissociation constant was 0.014 $\pm$ 0.002 min^{-1}.

J Nucl Med 1991; 32:000–000

There is ample evidence from both experimental and clinical studies that changes in beta-adrenergic receptor density can be associated with cardiac diseases, such as congestive heart failure, myocardial ischemia and infarction, cardiomyopathy, diabetes, or thyroid-induced heart muscle disease. Changes in beta-adrenergic density have also been shown in the denervated transplanted heart (1, 2). These alterations of cardiac adrenoceptors have been demonstrated in vitro on homogenates from samples collected mainly during surgery or postmortem.

Recent developments of positron emission tomography (PET) and of radioligands suitable for in vivo cardiac receptor binding studies make both the imaging and the

quantification of receptor density possible (1,2). Important information in the living physiologic and pathologic conditions, as well as in defining the alterations induced by treatment of certain diseases, are thus now available.

The most commonly used beta-adrenergic ligands in in vitro binding studies are lipophilic antagonists such as [^{125}I]iodocyanopindolol, [^{3}H]dihydroalprenolol, or [^{125}I]iodopindolol. However, the hydrophilic antagonist, [^{3}H] CGP 12177, has proved to be superior in studies with intact cells, and particularly in studies of the agonist-induced internalization of beta-adrenergic receptors (3,4). [^{3}H]CGP 12177 binds to the receptor in crude membranes or intact cells with a very high affinity (0.3 nM) (5). Owing to its high hydrophilicity, [^{3}H]CGP 12177 selectively identifies cell-surface beta-receptors that are thought to be coupled to adenylate cyclase.

We previously showed that lipophilic molecules such as [^{11}C]propranolol could not be used for studying the cardiac beta-adrenoceptor with PET because it accumulates in the lungs after intravenous injection during time of PET imaging (1). Carbon-11-practolol, a hydrophilic ligand, concentrated in the heart, but its low affinity prevented measurement of receptor density (1). It could be anticipated that because of both its very high hydrophilicity and affinity [^{11}C]CGP 12177 would bind to myocardial β-adrenergic receptors with low nonspecific binding to the heart and lung tissue.

The concentration of receptor sites cannot be directly deduced from measured PET radioactive concentration values and it is necessary to use a mathematical model. The model parameters, including the receptor concentration and the kinetic rate constants, can be identified from experimental data using either the kinetic method or a graphical method. The kinetic method is based on a fitting procedure, allowing the identification of all the model parameters which makes this method available even with a complex model. The main constraints of these fitting procedures are the need to measure the input function (usually the labeled ligand concentration in the arterial plasma) and to maintain a balance between the respective

complexities of the model structure and of the experimental protocol (6). This is not always possible if we wish to consider a complex model and if the choice of experimental protocol is too limited. The graphical methods only give some parameter values and are based on simplifying hypotheses, very simple models or special protocols. Often, these graphical methods only allow the identification of a composite parameter such as the product of the association rate constant and the receptor concentration (7).

In this study, we have envisaged the two approaches. However, the fitting method, as suggested in (6,8), appears difficult to use because of the presence of metabolites which make the input function difficult to measure and also inaccurate. So, we propose an original graphical method based on a special protocol and on certain hypotheses which are justified in the case of CGP 12177. With this method we can obtain the concentration of beta-adrenergic receptor sites in vivo without having to measure the input function and the metabolites.

MATERIALS AND METHODS

Animal Preparation

Male or female beagle dogs, weighing 10–12 kg were fasted overnight before the experiment. They were anesthetized first with a bolus of sodium thiopental (25 mg/kg) followed by a continuous injection at a rate of 5 mg/kg/hr. All dogs had undergone an endotracheal intubation and were ventilated with room air by a respirator (Monnal D Medical). A catheter to inject the ligand was inserted in the right atrium via the jugular vein, while a second catheter was inserted into the aorta via a femoral artery to withdraw arterial blood. The animals were monitored continuously by an electrocardiogram.

Preparation of (±)[^{11}C]CGP 12177

4-(3-t-butylamino-2-hydroxypropoxy)-benzimidazol-one ((±) CGP 12177) was labeled with carbon-11 using CGP 17704 as a precursor and [^{11}C]phosgen (9). Labeled material was purified using high-performance liquid chromatography, the specific radioactivity varying from 400 to 1300 mCi/μmole (15 – 48 GBq/μmole) at the time of injection.

Plasma Radioactive Concentration Measurements.

Arterial blood samples were collected from the aorta when the measurement of the plasma time-activity curve, $C_a^*(t)$, was necessary. After rapid centrifugation of sampled blood, the ^{11}C radioactive concentration in plasma was measured in a gamma counting system (Kontron CG 4000). The time-activity curves were corrected for physical decay of ^{11}C activity from time T_0. Plasma concentrations were expressed as pmole/ml after dividing by the specific radioactivity.

Metabolite Measurement Methods

The experimental process used for measuring the concentration of unmetabolized (±)[^{11}C]CGP 12177 has been described (10). About 50–80 mCi (1.8–3 GBq) of (±)[^{11}C]CGP 12177 were intravenously injected and blood samples were collected between 1 and 30 min. Plasma radioactive concentrations were measured after centrifugation. For the measurement of unchanged labeled CGP in plasma, 2 ml of methanol were added to 0.2 ml of plasma. After centrifugation, the precipitate was resuspended and

washed in 1 ml of methanol. After the methanolic supernatant was evaporated, the residue was dissolved with 20 μl of methanol and analyzed by thin-layer chromatography (TLC) on silica gel (Si60 F254, Merck) and on reverse-phase support (RP18 F254, Merck). Ascending free migration or over-pressure liquid chromatography was used to separate radioactive compounds which were measured using a radiochromatogram analyzer.

PET Measurements

PET studies were performed using a seven-slice, time-of-flight assisted positron camera (11) (LETI TTV01, Commissariat à l'Energie Atomique, Grenoble, France). Each slice was 13 mm thick and spatial transverse resolution was 12 mm. Transmission scans were performed with a rotating ^{68}Ge source to correct emission scans for 511 keV photon gamma-ray attenuation through the thorax. Emission data were recorded in list mode starting with the first injection of [^{11}C]CGP 12177 until the end of the experiment.

Sequential images, from one of the seven cross sections intersecting the ventricular septum, were selected for analysis. Outer myocardial boundaries were automatically defined with an iso-contour plotting routine. The 80% isocontour which was selected on a 20-min image included the septum and the left ventricular wall. Radioactivity was measured in each region of interest after correction for ^{11}C decay and expressed as pmole/ml after normalization using the specific radioactivity measured at time T_0. Calibration was performed every week by the use of a cylindrical phantom containing a uniform source of ^{68}Ge.

Myocardial wall thickness was measured postmortem and PET data were corrected for count recovery loss. This loss was due to the small size of the heart wall compared to the spatial resolution of PET. This correction was performed using a recovery factor measured experimentally on a heart phantom with the same PET system. The thickness of the ventricular septum and lateral wall of the left ventricle was measured after death and was found to be 10 ± 0.2 mm (12). The ratio of true-to-measured concentration was equal to 0.45 for a 10-mm thickness in our phantom calibration experiments. True [^{11}C]CGP 12177 concentrations were obtained by dividing the measured concentration values by this 0.45 recovery coefficient.

Experimental Protocol

The protocol included three injections of [^{11}C]CGP 12177 and/or CGP 12177. A trace dose, D_0^*, of [^{11}C]CGP 12177 was intravenously injected for about 1 min at the beginning of the experiment (time T_0). At time T_1, we injected a mixture of labeled and unlabeled CGP 12177 in the same syringe ("co-injection" experiment). The injected amounts of labeled and unlabeled ligand were denoted by D_1^* and D_1, respectively. [^{11}C]CGP 12177 injected at T_0 and T_1 was produced by the same synthesis so that the specific radioactivity measured at T_0 was identical for both injections. At time T_2, a third injection, consisting of an additional intravenous injection of an excess of unlabeled ligand (dose D_2), was performed ("displacement" experiment). Exact timing and doses administered during the five experiments are given in Table 1.

The Ligand-Receptor Model

The in vivo kinetics of labeled CGP 12177 between blood and beta-adrenergic receptor sites are composed of two basic processes. First, the free ligand is transferred from plasma to tissue, and second, the ligand binds to available free receptor sites.
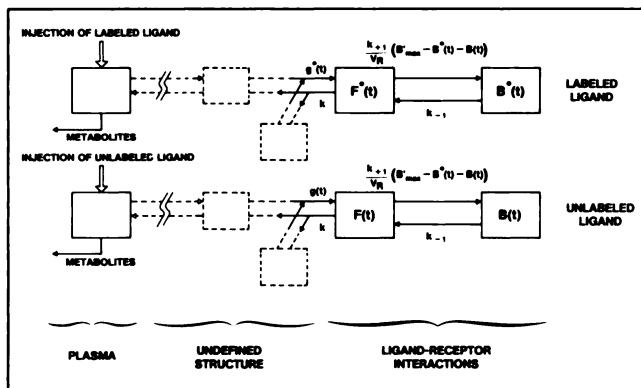
FIGURE 1. Compartmental ligand-receptor model used to estimate the concentration of receptor by a graphical method. The upper part represents the possible model describing the kinetics of the radioligand (quantities denoted with a star superscript) and the lower part, the same model associated with the unlabeled ligand (quantities denoted without a star superscript). The structure of this model is undefined except for the part concerning the ligand-receptor interactions which includes the free ligand compartment concentration (F or F*) and the bound ligand compartment concentration (B or B*). All transfer kinetics between compartments are linear except for the binding probability which depends on the biomolecular association rate constant and on the local concentration of free receptor sites. The PET data represent the sum of the concentrations of the labeled ligand in all compartments. The unlabeled ligand is not directly observable with PET, but the concentration of the unlabeled bound ligand has an effect on the local concentration of free receptor sites and consequently on the binding probability of free radioligand.

The ligand-receptor interaction is considered to be similar in both the in vivo and in vitro approach (2). We assume that a boundary layer, containing free ligand at a given concentration, F*(t), is formed in the interstitial space close to the myocardial cells (13). The free ligand may bind directly to a free receptor site, escape to other compartments, or possibly bind nonspecifically (Fig. 1). We may also include the nonspecific and reversible binding in the free ligand compartment, F*, if the association-dissociation kinetic rate constants are much higher than the other rate constants (14,15). In a simple case where the ligand binds reversibly to a single class of independent sites, the specific binding probability depends on the bimolecular association rate constant and on the local concentration of free receptor sites, which is equal to [B'_{max} − B*(t)], where B'_{max} is the unknown concentration of free receptor sites available for binding and B*(t) is the concentration of labeled ligand bound to receptors. The association rate constant is denoted by k_{+1}/V_R (as ml pmole^{-1} min^{-1}), where V_R (as ml/ml) is the volume of reaction defined as the fraction of the region of interest in which the ligand can react with receptors (6). The rate constant for the dissociation of the bound ligand is denoted by k_{-1}. The ratio of k_{-1} to k_{+1} defines the equilibrium dissociation constant K_d.

The number of compartments and the model structure representing the transfer of the free ligand from plasma to tissue may differ depending on the human organ, the molecule, or the experimental protocol used [see detailed and critical reviews of the quantitative models in refferences (6,7,13-17). In the model diagram represented in Figure 1, the sum of the transfer constants from the free ligand in the boundary layer (concentration F*(t))

to all other compartments, except to the bound ligand compartment, is denoted by k. The flux of labeled ligand in the opposite direction is denoted by g*(t).

The protocol included injections of unlabeled ligand during displacement and coinjection experiments. The kinetics of the unlabeled ligand are not seen directly by PET data, but they affect the local concentration of free receptor sites and thus the kinetics of the labeled ligand. Therefore, the kinetics of the unlabeled ligand must be taken into account in the model. The notations indicating the concentration of the unlabeled ligand are similar to those used for the labeled ligand but without an asterisk.

The ligand-receptor kinetics, shown in the model diagram in Figure 1, is described by the following equation system, which presents two sets of two equations representing the labeled and unlabeled ligand kinetics (6):

$$\frac{dF^*(t)}{dt} = g^*(t) - k\ F^*(t) - \frac{k_{+1}}{V_R}$$
$$\cdot\ [B'_{max} - B^*(t) - B(t)]F^*(t) + k_{-1}B^*(t) \quad \text{Eq. 1}$$

$$\frac{dB^*(t)}{dt} = \frac{k_{+1}}{V_R}\ [B'_{max} - B^*(t) - B(t)]F^*(t) - k_{-1}B^*(t) \quad \text{Eq. 2}$$

$$\frac{dF(t)}{dt} = g(t) - k\ F(t) - \frac{k_{+1}}{V_R}$$
$$\cdot\ [B'_{max} - B^*(t) - B(t)]F(t) + k_{-1}B(t) \quad \text{Eq.3}$$

$$\frac{dB(t)}{dt} = \frac{k_{+1}}{V_R}\ [B'_{max} - B^*(t) - B(t)]F(t) - k_{-1}B(t) \quad \text{Eq. 4}$$

$$F^*(0) = B^*(0) = F(0) = B(0) = 0 \quad \text{Eq. 5}$$

The unlabeled ligand kinetics were assumed to be similar to those of the labeled ligand. Thus, the model structure and the parameter values are the same in both parts of this model (see Fig. 1).

Hypotheses

The proposed method can only be used if the myocardial time-activity curve rapidly becomes a straight line on a logarithmic scale after injecting the labeled ligand. We were able to distinguish from our experiments the fast kinetic periods (between the time of a labeled ligand injection and the beginning of a straight line) and the slow kinetic periods (represented by a straight line). With the proposed protocol, we had two fast kinetic periods and three slow kinetic periods (Figs. 2 and 3). This graphical method is based on the model diagram shown in Figure 1 and on four hypotheses; three related to the kinetics of the ligand (Hypotheses 1-3) and one to the injected doses (Hypothesis 4).

Hypothesis 1: During a slow kinetic period, the measured PET concentrations principally representd the bound radioligand concentration.

Hypothesis 2: The dissociation rate constant was sufficiently low so that the dissociations can be neglected during a fast kinetic period.

Hypothesis 3: The function F*(t) (or F(t)) indicated that the free ligand concentration was equal to the product of the injected dose of labeled (or unlabeled) ligand by a unknown function $F_i(t)$, assumed to represent the free ligand concentration obtained after an injected dose equal to 1 nM.

Hypothesis 4: After the first injection (a trace amount of labeled ligand), the labeled bound ligand concentration (B*(t))
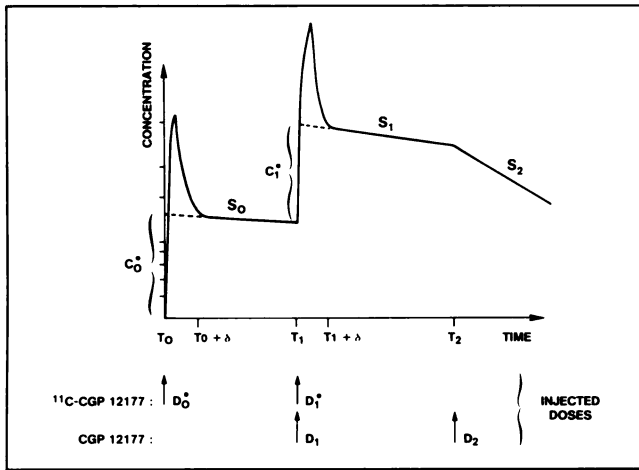
FIGURE 2. Schematic representation of a myocardial time-concentration curve showing the graphical measurements. The experimental protocol is defined by the injection times (T_0, T_1, and T_2) and by the injected doses of [^{11}C]CGP (D_i with star superscript) or unlabeled CGP (D_i without star superscript). The measurements of the two concentrations, C_0^* and C_1^*, are sufficient to estimate the concentration of available receptor sites B_{max}'. The use of the three slopes S_0, S_1 and S_2 allows the estimation of the dissociation rate constant and the composite parameter $k_{+1}/(k.V_R)$ (See text).

was negligible compared to B_{max} and after the second injection (a mixture of labeled or unlabeled ligand), it is negligible compared to the concentration of the receptor sites occupied by the unlabeled ligand. This hypothesis, which was easily verified using well-chosen injected doses, was very useful for simplifying the calculations. However, this hypothesis was not essential and the results were also given without it.

The validity of these hypotheses has been justified for CGP 12177 as shown in the Discussion section.

Graphical Determination of the Receptor Density

In order to estimate the receptor concentration, we used two experimental myocardial concentration values obtained from the
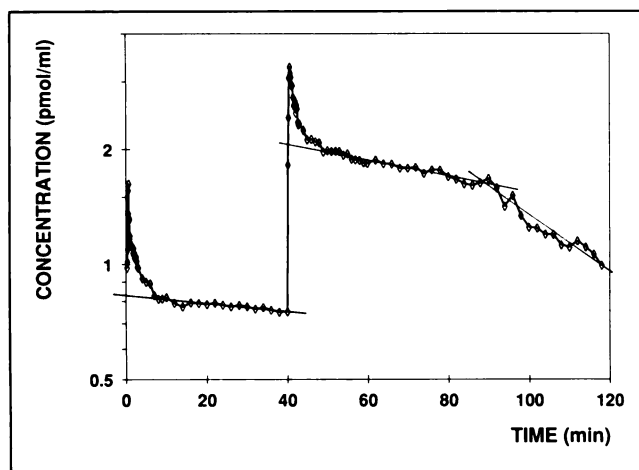

FIGURE 3. Example of the myocardial time-activity curve following injection of (±)[^{11}C]CGP 12177. Exact timing, doses, and results are given in Tables 1 and 2 (experiment 1).

PET time-activity curve. First, C_0, which represents the intercept at the concentration axis of the straight line on a logarithmic scale corresponding to the slow kinetics following the first injection. Second, C_1^*, which represents the difference between the concentration at T_1, extrapolated from the straight line obtained after the second injection, and the concentration measured just before this second injection (Fig. 2).

The proposed graphical method estimated the receptor concentration using five values: the two measured concentrations C_0^* and C_1^*, and the three doses D_0^*, D_1^*, and D_1, which was the labeled or unlabeled CGP 12177 injected at time T_0 and T_1.

The first injection being a tracer injection, the concentration $B^*(t)$ was very low compared to B_{max}' (Hypothesis 4). Therefore, we can consider the model as a linear model with a binding rate constant equal to $k_{+1}B_{max}'/V_R$. The function, $F^*(t)$, the evolution of the concentration of the free labeled ligand in the boundary layer, was an unknown function, but we assumed that it became negligible after a fast kinetic period (Hypothesis 1). Consequently, by integrating Equation 2 and ignoring the dissociation of the bound ligand ($k_{-1}B^*(t)$) (Hypothesis 2), we obtained the following equation:

$$B^*(\delta) = \frac{k_{+1}}{V_R}B_{max}'\int_0^\delta F^*(\tau)d\tau, \qquad \text{Eq. 6}$$

where δ represents the duration of the fast kinetic period. From Hypothesis 3, we have for any injected dose D_0^*:

$$\int_0^\delta F^*(\tau)d\tau = \gamma D_0^*, \qquad \text{Eq. 7}$$

where

$$\gamma = \int_0^\delta F_1(\tau)d\tau. \qquad \text{Eq. 8}$$

The measured concentration C_0^* corresponds about to $B^*(\delta)$ (Hypothesis 1) and therefore we deduced from Equations 6 and 7 that C_0^* can be written as:

$$C_0^* = k_{+1}\gamma B_{max}'D_0^*/V_R, \qquad \text{Eq. 9}$$

and therefore

$$\gamma = \frac{C_0^* V_R}{k_{+1}B_{max}'D_0^*}. \qquad \text{Eq. 10}$$

At time T_1, we injected both labeled and unlabeled ligand. Since the injected unlabeled ligand quantity was much greater than the injected labeled ligand quantity, we consider, the labeled ligand as a tracer of the unlabeled ligand kinetics (Hypothesis 4). Therefore, from C_1^*, which was assumed to be an estimation of the labeled bound ligand concentration (Hypothesis 1) resulting from the second injection, we can estimate the concentration C_1 of the unlabeled bound ligand by the following equation:

$$C_1 = C_1^*\frac{D_1}{D_1^*}. \qquad \text{Eq. 11}$$

The value of C_1 can also be calculated using another way. Since $B^*(t)$ is negligible compared to $B(t)$ (Hypothesis 4) and since the dissociation of the bound ligand ($k_{-1}B(t)$) can be ignored during a fast kinetic period (Hypothesis 2), we deduced from Equation 4 that the binding kinetics of the unlabeled ligand

during the period $[T_1, T_1 + \delta]$ was described by the following equation:

$$\frac{dB(t)}{dt} = (k_{+1}/V_R)(B'_{max} - B(t))F(t), \quad t\in[T_1, T_1 + \delta] \qquad \text{Eq. 12}$$

$$B(T_1) = 0 \qquad \text{Eq. 13}$$

The solution of this differential equation is given by:

$$B(t) = B'_{max}\left(1 - e^{-(k_{+1}/V_R)\left(\int_{T_1}^{t} F(\tau)d\tau\right)}\right)$$

$$t\in[T_1, T_1 + \delta]. \qquad \text{Eq. 14}$$

Similar to the equivalence between C^*_0 and $B^*(\delta)$, we can consider that C_1 corresponds about to $B(T_1 + \delta)$. Therefore, a second estimation of C_1 was obtained:

$$C_1 = B'_{max}\left(1 - e^{-(k_{+1}/V_R)\left(\int_{T_1}^{T_1+\delta} F(\tau)d\tau\right)}\right). \qquad \text{Eq. 15}$$

From Hypothesis 3, and similarly from Equation 7, we know that

$$\int_{T_1}^{T_1+\delta} F(\tau)d\tau = \gamma D_1. \qquad \text{Eq. 16}$$

From Equations 15 and 16, we found that

$$C_1 = B'_{max}(1 - e^{-k_{+1}\gamma D_1/V_R}). \qquad \text{Eq. 17}$$

Comparing Equations 11 and 17 and eliminating γ by Equation 10, finally led to the following equation:

$$B'_{max}\left(1 - e^{-\frac{C^*_0 D_1}{B'_{max}D^*_0}}\right) - C^*_1\frac{D_1}{D^*_1} = 0. \qquad \text{Eq. 18}$$

In this equation, all values were known except B'_{max}, which appeared twice. The unique solution of this equation which is of the type "$[f(B'_{max}) = 0$" can easily be obtained using a numerical or a graphical method.

If Hypothesis 4 cannot be consider as verified, similar calculations led to the more complex equation:

$$(B'_{max} - C^*(T_1 - \epsilon))$$

$$\left(1 - e^{\left(\frac{D^*_1+D_1}{D^*_0}\right)\log\left(\frac{B'_{max}-C^*_0}{B'_{max}}\right)}\right) - C^*_1\frac{D_1}{D^*_1} = 0, \qquad \text{Eq.19}$$

where $C^*(T_1 - \epsilon)$ is the concentration of the labeled CGP just before the second injection.

Determination of k_{-1} and $k_{+1}/(kV_R)$

We have assumed that the PET concentration principally represents the labeled bound ligand during the slow kinetic periods (Hypothesis 1). Therefore, the slopes of the straight line on a logarithmic scale were a function of the number of the occupied receptor sites and of several kinetic rate constants (13).

After the first injection, the concentration of bound ligand was C^*_0, which was low when compared to the total number of receptors B'_{max} (Hypothesis 4). Therefore, the slope S_0 was very low and was given by the following equation:

$$S_0 = k_{-1}\frac{k}{k + (k_{+1}/V_R)B'_{max}}. \qquad \text{Eq. 20}$$

Just after the second injection, the concentration of unlabeled bound ligand C_1 was given by Equation 10. If the concentration of labeled bound ligand is considered negligible when compared to C_1 (Hypothesis 4), the slope S_1 is given by:

$$S_1 = k_{-1}\frac{k}{k + (k_{+1}/V_R)\left(B'_{max} - C^*_1\frac{D_1}{D^*_1}\right)}. \qquad \text{Eq. 21}$$

The third injection was an injection of a large amount of unlabeled ligand, and we can consider that all the receptor sites were occupied. Therefore, from the slope S_2, we immediately deduced an estimation of the dissociation rate constant k_{-1}:

$$k_{-1} = S_2. \qquad \text{Eq. 22}$$

From Equations 20-22, we calculated two estimations of the ratio $k_{+1}/(k.V_R)$ using the following equations:

$$\frac{k_{+1}}{k.V_R} = \left(\frac{S_2}{S_0} - 1\right)\frac{1}{B'_{max}} \qquad \text{Eq. 23}$$

$$\frac{k_{+1}}{k.V_R} = \left(\frac{S_2}{S_1} - 1\right)\frac{1}{\left(B'_{max} - C^*_1\frac{D_1}{D^*_1}\right)} \qquad \text{Eq. 24}$$

RESULTS

Myocardial and Plasma Time-activity Curves

Five dog experiments were performed according to the experimental protocol previously described using three injections. The time-concentration curves of labeled ligand in the myocardium reached a maximum (0.92 ± 0.07 pmole/ml^{-1} per nM injected) within the first minute following the first injection. Then, the curves fell rapidly and during the period (8 min, T_1) they presented a plateau at a level of 0.46 ± 0.03 pmole/ml^{-1} per nM injected, with a low slope estimated at 0.0044 ± 0.0015 min^{-1} (Fig. 3). The same phenomenon was observed after the second injection, the slope of the curve appeared constant on a logarithmic scale during the period $[T_1 + 8$ min, $T_2]$ (0.0059 ± 0.0005 min^{-1}). However, this second injection including unlabeled ligand, and the height of the second plateau (C^*_1) was lower than the height of the first (C^*_0), depending on the injected amount D_1 of the unlabeled CGP. This ratio C^*_1/D^*_1 was respectively 0.242 and 0.247 pmole ml^{-1} per nM injected in the two experiments using a dose D_1 equal to 0.025 mg (Exp. 1 and 2), and it was respectively 0.289, 0.302, and 0.366 when D_1 was respectively equal to 0.020 mg (Exp. 5), 0.015 mg (Exp. 3), and 0.010 mg (Exp. 4). The injection of an excess of unlabeled ligand (injection 3) at time T_2 led to a significant modification of the curve slopes which became steeper (0.0137 ± 0.0018 min^{-1}).

No significant change in canine heart rate was observed during continuous monitoring, even after the largest amounts of CGP were injected.

Metabolite Study

An experiment was performed with a single injection of 2.5 mCi (0.092 GBq) of [^{11}C]CGP 12177 with high-specific activity (380 mCi/μmole, 14 GBq/μmole), which also included the measurement of the plasma concentration (Fig. 4). The time-concentration curve of labeled ligand in the plasma had a maximum (25.7 pmole/ml) within the first minute. It then fell rapidly but remained significant throughout the experiment: 2.3 pmole/ml at 10 min and 0.8 pmole/ml at 50 min. The myocardial concentration measured by PET had a smaller maximum (5.8 pmole/ml) and it appeared constant (about 4 pmole/ml) during the 8–50-min period whereas the plasma concentration was divided by about three.

The comparison of radioactivity in the protein precipitate and the corresponding untreated plasmatic sample showed that more than 90% of the radioactivity was collected in methanol from plasma and analyzed by TLC. Radiochromatogram analysis obtained in normal and reverse phases were similar. These measurements showed that the labeled CGP metabolites appeared very quickly, the fraction of unmetabolized CGP ranging from 10% to 15% at 5 min and less than 5% at 20 min. Figure 5 displays a typical radio-TLC silica gel analysis that provides a way of estimating of the percentage of unmetabolized CGP 12177 in plasma. In Figure 4, the single injection experiment, the plasma concentration of unmetabolized CGP 12177 was traced, which allowed the comparison of this curve with the plasma concentration without correction.
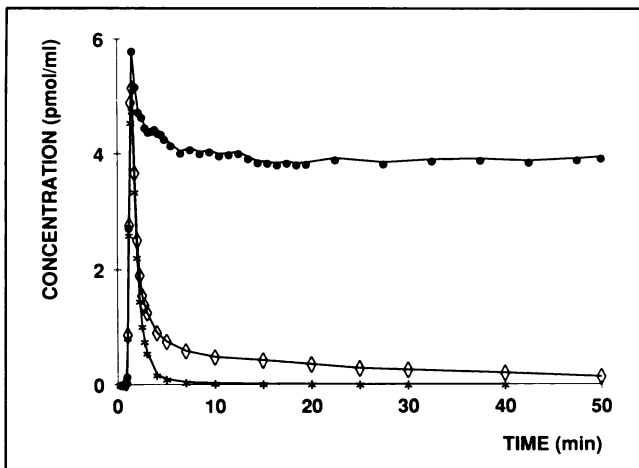

FIGURE 4. Example of the myocardial and plasma time-activity curves following a single injection of (±)[^{11}C]CGP 12177. (●): Concentration of labeled CGP in dog heart measured by PET. (◇ × 5): Arterial plasma radioactive concentration uncorrected for metabolites. (★ × 5): Plasma concentration of unmetabolized (±)[^{11}C]CGP 12177. During the period 5–50 min, the myocardial concentration appeared almost constant, whereas the plasma radioactive concentration was divided by three. Since the plasma concentration of unmetabolized CGP appeared negligible after 5 min, these results suggest that this last curve is much closer to the true input function than the uncorrected plasma radioactivity curve.
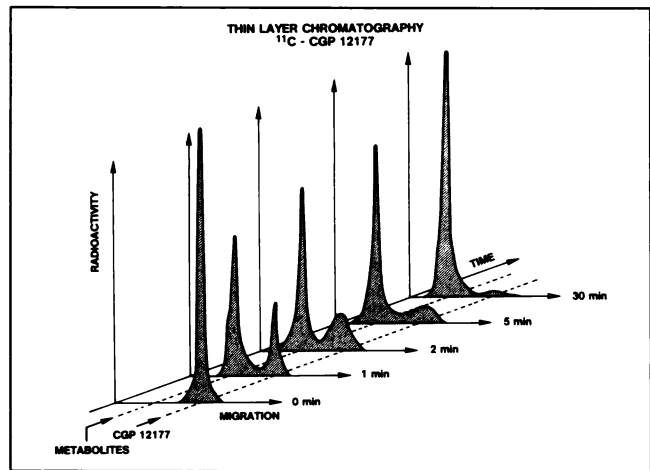

FIGURE 5. Typical radiochromatogram obtained after TLC silica gel analysis. These results showed that the labeled (±)CGP 12177 metabolites appeared very quickly. The fraction of unmetabolized (±)CGP 12177 ranged from 10% to 15% at 5 min and less than 5% at 30 min.

Beta-Adrenergic Receptor Density and Kinetic Rate Constants

Table 1 gives the detailed timing, the injected doses, and the concentrations (C_0^* and C_1^*) measured in all five experiments. In the first three experiments, the two injected labeled CGP doses (D_0^* and D_1^*) were almost similar. In the two other experiments, the dose D_1^* was two or three times larger than the first dose D_0^* in order to compensate for the increase of the experimental uncertainties associated with ^{11}C decay during the second slow kinetic period. In the same experiments, the times between the three injections were longer in order to improve the accuracy of the S_0 and S_1 slopes.

Two estimations of the receptor concentration B_{max}' are given in Table 1. The first estimation was obtained by solving Equation 18, the second by solving Equation 19. Hypothesis 4 only needs to be verified in the first case. The means and the usual standard deviations were calculated from the five experiments. The results obtained from the two equations were similar (Table 1): it was found that B_{max}' was 30.9 ± 3.7 pmole/ml tissue with Hypothesis 4 and 29.4 ± 3.4 pmole/ml tissue without this hypothesis.

Table 2 gives the slopes P_1, P_2, and P_3 graphically measured and the estimations of parameter k_{-1} and of the composite parameter $k_{+1}/(k.V_R)$ deduced from Equations 22 and 23. The dissociation rate constant k_{-1} was found to be equal to 0.014 ± 0.002 min^{-1}. The parameter $k_{+1}/(k.V_R)$ was estimated to 0.10 ± 0.07 min^{-1} when the slopes S_0 and S_2 were used (Equation 22) and 0.17 ± 0.04 min^{-1} when the slopes S_1 and S_2 were used (Equation 23).

DISCUSSION

We have previously shown that the hydrophilic compound (±)[^{11}C]CGP 12177 met all the criteria needed to characterize the specific binding of a ligand to its receptor

TABLE 1
Numerical Values of the Protocol Parameters (Injection Times and Injected Doses) of the Two Concentration Graphical Measurements and of the B'_{max} Estimations Corresponding to the Five Experiments Performed.

	Units	Exp. 1	Exp. 2	Exp. 3	Exp. 4	Exp. 5	Means ± s.d.
S.A.	mCi/μM	933	392	820	1318	1070	
Timing and injected doses							
Initial Injection ($T_0 = 0$)							
$D^{\ast}_0$	nM	4.8	9.4	3.5	1.7	1.9	
Coinjection							
T_1	min	30	30	30	40	40	
$D^{\ast}_1$	nM	5.6	6.9	3.7	3.6	5.9	
D_1	mg		0.025	0.015	0.010	0.020	0.025
Displacement							
T_2	min	70	70	70	90	90	
D_2	mg	6	6	1	1	1	
Exp. Dur.	min	100	100	100	120	120	
Concentration graphical measurements							
$C^{\ast}_0$ ± s.e.	pmole ml⁻¹	2.21 ± 0.02	3.65 ± 0.03	1.74 ± 0.02	0.82 ± 0.06	0.91 ± 0.02	
$C^{\ast}_1$ ± s.e.	pmole ml⁻¹	1.39 ± 0.13	1.71 ± 0.19	1.12 ± 0.12	1.32 ± 0.06	1.71 ± 0.02	
Estimations of B'_{max}							
With Hypothesis 4 (Eq. 18)							
B'_{max} ± s.e.	pmole ml⁻¹	30.2 ± 5.4	35.4 ± 11.9	24.5 ± 6.7	33.7 ± 8.2	31.0 ± 5.1	30.9 ± 3.7
Without Hypothesis 4 (Eq. 19)							
B'_{max} ± s.e.	pmole ml⁻¹	30.9 ± 4.9	34.7 ± 8.9	24.6 ± 5.6	27.4 ± 4.4	29.5 ± 4.2	29.4 ± 3.4

S.A. = specific activity measured at T_0.
s.e. = standard errors. The standard errors of $C^{\ast}_0$ and $C^{\ast}_1$ have been estimated using the classical approach based on the least-squares method (see ref. 6). The standard errors of B'_{max} are obtained by a Monte-Carlo method.
s.d. = Usual standard deviation calculated from the five experiments.

TABLE 2
Numerical Values of the Slope Graphical Measurements and of Two Kinetic Parameters Corresponding to the Five Experiments Performed

	Units	Exp. 1	Exp. 2	Exp. 3	Exp. 4	Exp. 5	Means ± s.d.
Slope graphical measurements							
S_0 ± s.e.	min⁻¹	0.0033 ± 0.0005	0.0048 ± 0.0005	0.0066 ± 0.0007	0.0021 ± 0.0003	0.0054 ± 0.0005	0.0044 ± 0.0015
S_1 ± s.e.	min⁻¹	0.0058 ± 0.0004	0.0062 ± 0.0011	0.0068 ± 0.0006	0.0053 ± 0.0003	0.0057 ± 0.0005	0.0059 ± 0.0005
S_2 ± s.e.	min⁻¹	0.0113 ± 0.0005	0.0154 ± 0.0013	0.0116 ± 0.0010	0.0153 ± 0.0014	0.0147 ± 0.0026	0.0137 ± 0.0018
Results							
k_{-1} ± s.e.	min⁻¹	0.0113 ± 0.0005	0.0154 ± 0.0013	0.0116 ± 0.0010	0.0153 ± 0.0014	0.0147 ± 0.0026	0.0137 ± 0.0018
Estimation of $k_{+1}/(k.V_R)$ from S_0 and S_2 (Eq. 22)							
$k_{+1}/(k.V_R)$ ± s.e.	ml pmole⁻¹	0.08 ± 0.02	0.07 ± 0.03	0.04 ± 0.02	0.23 ± 0.07	0.06 ± 0.02	0.10 ± 0.07
Estimation of $k_{+1}/(k.V_R)$ from S_1 and S_2 (Eq. 23)							
$k_{+1}/(k.V_R)$ ± s.e.	ml pmole⁻¹	0.16 ± 0.10	0.15 ± 0.09	0.12 ± 0.09	0.16 ± 0.08	0.25 ± 0.14	0.17 ± 0.04

s.e. = standard errors estimated according to the classical approach based on the least-squares method (see ref. 6).
s.d. = usual standard deviation calculated from the five experiments.

site. A high ventricular myocardial uptake was seen in dogs and in normal volunteers after intravenous injection of a trace dose of $(\pm)[^{11}C]CGP$ 12177 (2,18). The rapid intravenous injection of an excess of cold CGP or pindolol, 26 min after the radioligand injection, led to rapid decrease in myocardial radioactivity. The percentage of radioligand displaced 30 min after injection of the excess of cold compound was related to the amount of cold CGP or pindolol injected for displacement and to the degree of the decrease in the heart rate. Both physiologic effect and binding inhibition were synchronous (2,18). The same patterns of inhibition were seen in the present study when increasing amounts of unlabeled CGP 12177 were injected at time T_1 and T_2.

The goal of this work was to measure the beta-adrenergic receptor density and the rate constants describing the binding kinetics in vivo using the same ligand. One of the principal advantages of CGP 12177 for in vivo cardiac studies is its low nonspecific binding because the fraction of nonspecific binding is much more difficult to evaluate in the heart than in the brain where one can often find some regions without receptor sites, e.g., the cerebellum when studying the D2 receptors (7,15). The other principal advantage is that CGP 12177 binds to plasma-membrane receptors and thus a decrease of receptors due to a movement of the receptors from the plasma membrane to a vesicular cell compartment can be detected although there is no change in the total number of receptor sites. A rapid decrease in the number of receptors detectable with CGP 12177 has been observed during the desensitization of the beta-adrenergic receptors (5). An externalization of beta-adrenergic receptors has been observed after 1 hr of myocardial ischemia in guinea pig and dog heart (19,20).

The Kinetic Approach and the Metabolites

We have investigated the possibility of modeling the interactions of the $(\pm)[^{11}C]CGP$ with cardiae beta-adrenergic receptors using data obtained from a single injection (Fig. 4). Using the plasma concentration values obtained from arterial samples as input function, we have tested all the classical models containing less than five parameters. However, with the linear models, the fits were never satisfactory. These simple models could not explain why, after an injection of $[^{11}C]CGP$ at high-specific activity, the PET concentration was constant or decreased very slowly during the 8–50-min period, whereas the plasma concentration was divided by three. We therefore suspected that the plasma curve was not representative of the input function in the myocardium. The only good fit was obtained with a non-linear model in which the receptor density was such that all receptors could be occupied 7 min after the initial tracer injection. This explanation seemed unacceptable, so we concluded that the stability of the PET concentration 8 min after an injection must be explained by the absence or a very slight transfer between the blood and the tissue. This supposes that the apparent

dissociation rate constant is very low and that the true input function becomes rapidly negligible.

The metabolite study showed that the metabolism of $(\pm)CGP$ 12177 was very fast and that the unmetabolized ligand concentration in the plasma disappeared 5 min after the injection. Therefore, the apparent disappearance of the transfers between blood and tissue at the same time, may be explained by the fact that metabolites enter the myocardium very slowly or do not enter it at all. The modeling of the myocardial time-concentration curve, using the unmetabolized labeled concentration in the plasma as input function, was tested. However, the uncertainties of the input function (difficult to estimate but probably about 50%) due to the measurement method, and the very small percentage of unmetabolized ligand, resulted in inaccurate identification of the model parameters (e.g. about 60% for B_{max} in the best cases).

The Graphical Method and its Hypotheses

This graphical method has the main advantage of not using an input function, which is possible because of Hypothesis 3. The unknown ratio from the integral of the free ligand concentration curve to the injected dose (coefficient γ in Equations 7 and 16) is eliminated by comparing the data after the first two injections. An important consequence of this method without input function is that the structure of the model between the plasma compartment and the free ligand compartment (F* or F) can remain unknown. For example, we have included an unknown number of intermediate compartments and a possible nonspecific binding compartment in Figure 2. Another advantage of the absence of an input function is that we do not have to measure the metabolites. Our assumption, that the CGP metabolites have difficulty entering the myocardium, is not essential and there is no inconvenience if a small percentage of metabolites reach the tissue, providing the percentage is similar after the first two injections. Similarly, the influence of the local myocardial blood flow is not taken into account, provided the condition of local blood flow is not modified between the first two injections.

This graphical method for estimating B_{max} is based on four hypotheses. The first hypothesis assumes that the PET data of a slow kinetic period correspond principally to the labeled ligand concentration. This is justified by the fact that after a fast kinetic period resulting from an injection of high-specific activity the concentration is constant (or with a slight decrease) and it can only be significantly modified by an injection of unlabeled ligand. During an experiment (Fig. 6), we studied the displacement curve over a long period (70 min). After an initial injection of 3.2 nM (0.12 GBq) of $[^{11}C]CGP$ 12177, an injection of an excess of unlabeled CGP 12177 (6 mg) was given 30 min later. The curve appears as a straight line on a logarithmic scale, from the displacement time right up to the end of the experiment. Seventy minutes after an injection of an
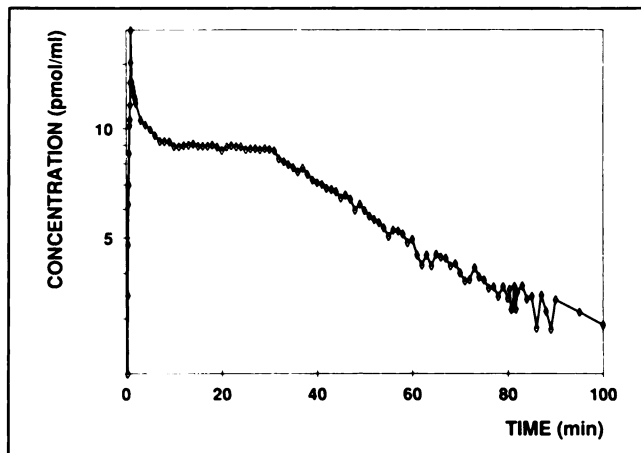
FIGURE 6. Example of a displacement experiment. After an initial injection of 3.2 nM (0.12 GBq) of (±)[^{11}C]CGP 12177, an injection of an excess of unlabeled CGP (6 mg) was performed at 30 min. The curve appears as a straight line on a logarithmic scale after the displacement time.

excess of unlabeled ligand, 70% of the unlabeled CGP was displaced. The short period of [^{11}C] does not allow the measurement of the undisplaceable fraction corresponding to a nonspecific binding, but previous studies showed that this fraction was small (*3,4*).

From the estimated value of the dissociation rate constant, we deduced that the maximum error, resulting from the neglect of the dissociations during a fast kinetic period (Hypothesis 2), was about 6.5%. However, taking into account the rebinding phenomenon (see later) and the fact that the concentrations C_0^* and C_1^* were extrapolated at times 0 and T_1, respectively (and not measured at the end of the fast kinetic periods), we estimate that the true error is about 1% or 2%.

The third hypothesis assumes that the free ligand concentration (curves $F(t)$ or $F^*(t)$), is the product at any time of the corresponding injected dose by the corresponding concentration given by a curve $F_1(t)$. This property is correct with a linear model and therefore entirely valid for the first tracer injection. After the second injection, the binding probability and thus the free ligand concentration depends on the concentration of receptor sites occupied by the unlabeled ligand. So, Hypothesis 3 is only an approximation if the percentage of occupied receptor sites is large. For example, the simulations showed that if 50% of the receptor sites were occupied at the end of the second fast kinetic period, the integral of the $F(t)$ corresponding to the unlabeled free ligand is underestimated by about 15% by Equation 16, which leads to an overestimation of B_{max}' of about 8%. This error can be decreased by reducing the dose D_1. However, since the estimation of B_{max}' is based on the comparison of the concentration between the first and the second slow kinetic periods, it is essential that the percentage of receptor sites occupied during the second period was significant. If it is too low, the bias introduced by Hypothesis 3 becomes negligible but the estimates of

the standard error become much greater. In practice, the percentage of the receptor sites occupied at the end of the second fast kinetic period 30%–50% seems to be the best solution, because the bias introduced by the Hypothesis 3 is much smaller than the standard error estimates.

The injection of [^{11}C]CGP 12177 cannot always be considered as a tracer injection. For example, in experiment 3, about 10% of receptor sites are occupied after the first injection. Therefore, the equation given the B_{max} value without Hypothesis 4 has been established (Equation 19). However, the comparison between the results obtained with and without this hypothesis (Table 1) shows that the differences are not significant.

Parameter Values

The density of beta-adrenergic receptors has been studied by in vitro methods and found to be different in each species. In biopsied specimens of the human left ventricle, the B_{max} was from 30 to 79 pmole/g of protein by [^{125}I] cyanopindolol (*21–23*), which equaled 152, 150, and 311 pmole/g of protein in the rat, rabbit, and dog, respectively, using [^{3}H]dihydroaprenolol (*24*). However, the results obtained by in vitro methods and by PET are difficult to compare since the first results are expressed as pmole/g of protein and the second as pmole/ml of tissue. Our result ($B_{max} = 29.4 \pm 3.4$ pmole/ml tissue) can be compared to the result obtained in dog using [^{3}H]dihydroaprenolol, if the percentage of tissue protein is estimated at 10%, which is a usual value.

The slopes of the curves after displacement showed that the dissociation rate constant is significant (0.0137 ± 0.0018 min^{-1}), indicating that about 1.4% of specifically bound ligand dissociated from the receptor sites every minute throughout the experiment. This is low but far from negligible. Therefore, the presence of a plateau, after the injection of ligand at high specific activity, is not an indication of the irreversibility of the ligand-receptor binding. It means that a ligand which dissociates from a receptor site has a higher probability of rebinding to the same or another free receptor site rather than escaping into capillary blood. From the obtained parameter values, we can estimate the probability of rebinding of a dissociated ligand by the ratio $(k_{+1}(B_{max}' - B^*(t) - B(t)))/(V_R k + k_{+1}(B_{max}' - B^*(t) - B(t)))$. It appears that this probability of rebinding is about 83% after the first injection (with a nonsignificant part of receptor sites occupied by (±)[^{11}C] CGP) and about 78% after the second (with about 50% of receptor sites occupied particularly by unlabeled CGP). The slight difference between these probabilities, in spite of the number of free sites divided by two, explains why the slopes S_0 (0.0044 ± 0.0015 min^{-1}) and S_1 (0.0059 ± 0.0005 min^{-1}) do not appear to be very different.

The affinity constant K_d cannot be identified by this approach since we can only estimate the composite parameter $K_d.k.V_R$, which is found to be equal to about 0.1 pmole ml^{-1} min^{-1}.

CONCLUSION

This study shows that it is possible to measure noninvasively beta-adrenergic receptor density in the living heart. It thus becomes possible to investigate possible changes in receptor density in patients. The relative insensitivity of the failing human heart to sympathetic stimuli could result in part from down-regulation of beta-adrenergic receptors, although a functional abnormality of the G stimulatory protein has also been demonstrated (25,26). Experimental myocardial ischemia provokes a rapid externalization of the beta-receptors by up to 50% (27) coupled to an increase in circulating catecholamines, which could explain the increased frequency of ventricular arrhytmias occurring after myocardial infarction. Beta blockade produces up-regulation of cardiac beta-receptors. These changes could be measured with PET and ^{11}C-CGP 12177 since this ligand binds only to cell surface receptors and is not internalized (5).

REFERENCES

1. Syrota A. Receptor binding studies of the living heart. *New Concepts Cardiac Imaging* 1988;4:141–166.
2. Syrota A. Positron emission tomography: evaluation of cardiac receptors. In: Marcus ML, Skorton DJ, Schelbert HR, Wolf GL, eds. *Cardiac imaging—principles and practice: a companion of Braunwald's heart disease* 1991: 1256–1270.
3. Staehelin M, Hertel C. [³H]CGP 12177: a β-adrenergic ligand suitable for measuring cell surface receptors. *J Receptor Res* 1983;3:35–43.
4. Staehelin M, Simons P, Jaeggi K, Wigger N. CGP 12177: a hydrophilic β-adrenergic receptor radioligand reveals high affinity binding of antagonist to intact cells. *J Biol Chem* 1983;258:3496–3502.
5. Hertel C, Muller P, Portenier M, Staehelin M. Determination of the desensitization of β-adrenergic receptors by [³H]CGP 12177. *Biochem J* 1983;216:669–674.
6. Delforge J, Syrota A, Mazoyer BM. Identifiability analysis and parameter identification of an in vivo ligand-receptor model from PET data. *IEEE Trans Biomed Eng* 1990;37:653–661.
7. Wong DK, Gjedde A, Wagner HN. Quantification of neuroreceptors in the living human brain. *J Cereb Blood Flow Metab* 1986;6:137–146.
8. Delforge J, Syrota A, Mazoyer BM. Experimental design optimization: theory and application to estimation of receptor model parameters using

dynamic positron emission tomography. *Phys Med Biol* 1989;34:419–435.
9. Boullais C, Crouzel C, Syrota A. Synthesis of 4-(3-t-butylamino-2-hydroxypropoxy)-benzimidazol-2(''C)-1 (CGP 12177). *J Label Compound Radiopharm* 1986;5:565–567.
10. Mazière B, Loc'h C, Stulzaft O. A new and rapid analytical procedure for measuring unchanged radiopharmaceuticals in blood and tissue samples. *J Label Compound Radiopharm* 1989;26:490–491.
11. Soussaline F, Comar D, Allemand R, Campagnolo R, Laval M, Vacher J. New developments in positron emission tomography instrumentation using the time-of-flight information. In: Greitz T, et al eds. *The metabolism of the human brain studied with positron emission tomography.* New York: Raven Press; 1985:1–11.
12. Charbonneau P, Syrota A, Crouzel C, Vallois JM, Prenant C, Crouzel M. Peripheral-type benzodiazepine receptors in the living heart characterized by positron emission tomography. *Circulation* 1986;73:476–483.
13. Syrota A, Paillotin G, Davy JM, Aumont MC. Kinetics of in vivo binding of antagonist to muscarinic cholinergic receptor in the human heart studied by positron emission tomography. *Life Sci* 1985;35:937–945.
14. Huang SH, Barrio JB, Phelps ME. Neuroreceptor assay with positron emission tomography: equilibrium versus dynamic approaches. *J Cereb Blood Flow Metab* 1986;6:515–521.
15. Perlmutter JS, Larson KB, Raichle ME, et al. Strategies for in vivo measurement of receptor binding using positron emission tomography. *J Cereb Blood Flow Metab* 1986;6:154–169.
16. Frey KA, Hichwa RD, Ehrenkaufer RLE, Agranoff BW. Quantitative in vivo receptor binding. III. Tracer kinetic modeling of muscarinic cholinergic receptor binding. *Proc Natl Acad Sci USA* 1985;82:6711–6715.
17. Logan J, Wolf AP, Shiue CY, Fowler JS. Kinetic modeling of receptor-ligand binding applied to positron emission tomographic studies with neuroleptic tracer. *J Neurochem* 1987;48:73–83.
18. Seto M, Syrota A, Crouzel C, et al. Beta-adrenergic receptors in the dog heart characterized by [''C]CGP 12177 and PET. *J Nucl Med* 1986;6:949.
19. Maisel A, Motulsky H, Insel P. Externalization of β-adrenergic receptors promoted by myocardial ischemia. *Science* 1985;230:183–185.
20. Vatner D, Knight D, Shen YT, Thomas J, Homcy C, Vatner S. One hour of myocardial ischemia in conscious dogs increases β-adrenergic receptors but decreases adenylate cyclase activity. *J Mol Cell Cardiol* 1988;20:75–82.
21. Stiles GL, Taylor S, Lefkowitz RJ. Human cardiac beta-adrenergic receptors: subtypes heterogeneity delineated by direct radioligand binding. *Life Sci* 1983;33:467–473.
22. Heitz A, Schwartz, Velly J. β-adrenoceptors of the human myocardium: determination of β₁ and β₂ subtypes by radioligand binding. *Br J Pharmacol* 1983;80:711–717.
23. Golf S, Lovstad R, Hansson V. β-adrenoceptor density and relative number of β-adrenoceptor subtypes in biopsies from human right atrial, left ventricular and right ventricular myocardium. *Cardiovasc Res* 1985;19:636–641.
24. Mukherjee A, Haghani Z, Brady J, et al. Differences in myocardial α- and β-adrenergic receptor numbers in different species. *Am J Physiol* 1983;245:H957–H961.
25. Fowler MB, Laser JA, Hopkins GL, Minobe W, Bristow MR. Assessment of the β-adrenergic receptor pathway in the intact failing human heart: progressive receptor down-regulation and subsensitivity to agonist response. *Circulation* 1986;74:1290–1302.
26. Feldman AM, Cates AE, Veazey WB, et al. Increase of the 40,000-mol wt pertussis toxin substrate (G protein) in the failing human heart. *J Clin Invest* 1988;82:189–197.
27. Maisel AS, Motulsky HJ, Insel PA. Externalization of beta adrenergic receptors promoted by myocardial ischaemia. *Science* 1985;230:183–186.